Human Molecular Genetics, 2013, Vol. 22, No. 3 **558–567**
doi:10.1093/hmg/dds466
Advance Access published on October 29, 2012

Gene therapy provides long-term visual function in a pre-clinical model of retinitis pigmentosa

Katherine J. Wert[1,2,3], Richard J. Davis[1,3], Javier Sancho-Pelluz[1,3], Patsy M. Nishina[4] and Stephen H. Tsang[1,3,5,*]

[1]Bernard & Shirlee Brown Glaucoma Laboratory, Departments of Ophthalmology, Pathology & Cell Biology, Columbia University, New York, NY 10032, USA, [2]Institute of Human Nutrition, College of Physicians & Surgeons, Columbia University, New York, NY 10032, USA [3]Edward S. Harkness Eye Institute, Columbia University, New York, NY 10032, USA [4]The Jackson Laboratory, 600 Main Street, Bar Harbor, ME 04609 and [5]New York-Presbyterian Hospital/Columbia University Medical Center, New York, NY 10032, USA

Received July 13, 2012; Revised October 18, 2012; Accepted October 24, 2012

Approximately 36 000 cases of simplex and familial retinitis pigmentosa (RP) worldwide are caused by a loss in phosphodiesterase (PDE6) function. In the preclinical *Pde6α*^{nmf363} mouse model of this disease, defects in the α-subunit of PDE6 result in a progressive loss of photoreceptors and neuronal function. We hypothesized that increasing PDE6α levels using an AAV2/8 gene therapy vector could improve photoreceptor survival and retinal function. We utilized a vector with the cell-type-specific *rhodopsin* (RHO) promoter: AAV2/8(Y733F)-*Rho-Pde6α*, to transduce *Pde6α*^{nmf363} retinas and monitored its effects over a 6-month period (a quarter of the mouse lifespan). We found that a single injection enhanced survival of photoreceptors and improved retinal function. At 6 months of age, the treated eyes retained photoreceptor cell bodies, while there were no detectable photoreceptors remaining in the untreated eyes. More importantly, the treated eyes demonstrated functional visual responses even after the untreated eyes had lost all vision. Despite focal rescue of the retinal structure adjacent to the injection site, global functional rescue of the entire retina was observed. These results suggest that RP due to PDE6α deficiency in humans, in addition to PDE6β deficiency, is also likely to be treatable by gene therapy.

INTRODUCTION

Loss of vision, leading to a loss of independence in activities of daily living resulting from some neurodegenerative diseases, such as retinitis pigmentosa (RP) or age-related macular degeneration (AMD), is due to photoreceptor cell death (1). In patients with RP, initially, death of the rod photoreceptors will cause night blindness. This is followed by a deterioration of the peripheral visual field and may progress until all visual response is extinguished. Approximately 36 000 cases of simplex and familial RP worldwide are caused by a mutation in the rod-specific cyclic guanosine monophosphate phosphodiesterase (PDE6) complex (2). In spite of the occurrence of this disease, no effective treatments are currently available to ameliorate this loss of vision.

The PDE6 complex is composed of catalytic (PDE6α and PDE6β) and regulatory (PDE6γ) subunits (3,4). There are several mouse models with mutations in the gene encoding the β-subunit, such as *Pde6β*^{rd1}, *Pde6β*^{rd10} and *Pde6β*^{H620Q}. These *Pde6β* mouse models have been useful for testing various drug and gene therapies, but in spite of this, most viral-mediated gene therapy approaches have met with limited success (5–12). Recently, an adeno-associated viral (AAV)2/8 gene therapy vector with a Y733F capsid mutation was shown to promote long-term rescue compared with the earlier AAV2 and AAV5 vector serotypes (13). Pang *et al.* improved visual function in the *Pde6β*^{rd10} mouse for 6 months using an AAV2/8 gene therapy vector.

Mouse models have been described with mutations in the gene encoding the α-subunit of PDE6; *Pde6α*^{nmf282} and *Pde6α*^{nmf363}, which have similar mutations found in human

*To whom correspondence should be addressed at: Edward S. Harkness Eye Institute, New York-Presbyterian/Columbia University Medical Center, 160 Fort Washington Ave. Research Annex, Room 513, New York, NY 10032, USA. Tel: +212 3421189; Fax: +212 3054987; Email: sht2@columbia.edu

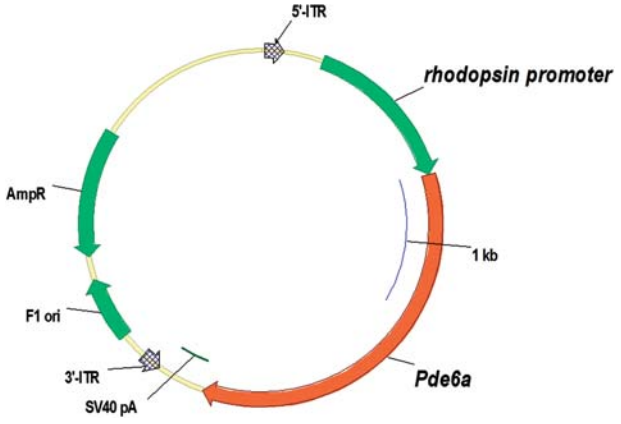

Figure 1. Schematic representation of the AAV2/8(Y733F)-*Rho-Pde6α* vector. pZac2.1 vector plasmid displaying the *Pde6α* complementary DNA (cDNA) fragment driven by 1.1 kb of the murine *rhodopsin* promoter. The Simian virus 40 (SV40) polyadenylation signal is located at the 3′ end of the cDNA. Arrows indicate the direction of transcription. 5′- and 3′-ITRs, inverted terminal repeat of AAV; AmpR, ampicillin-resistant gene; F1 ori, origin of replication. Scale bar: 1 kb.

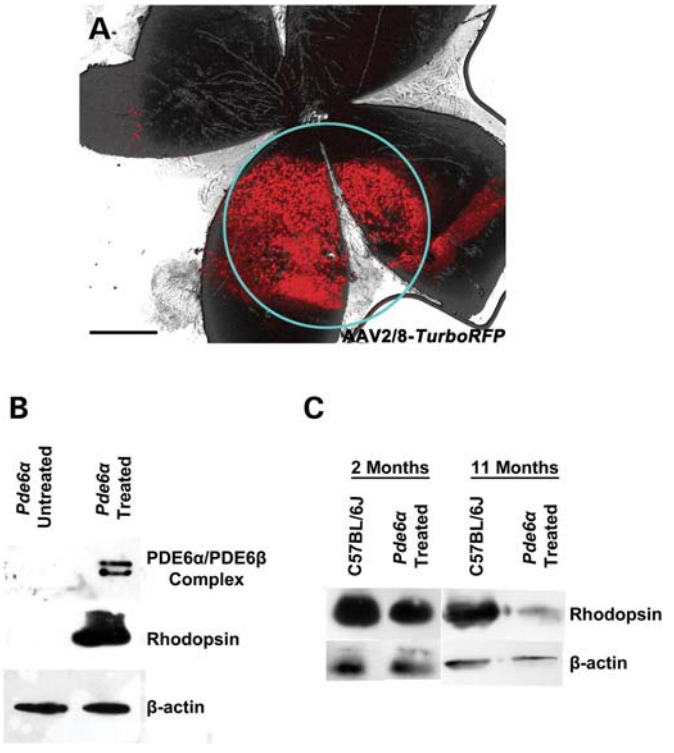

Figure 2. Viral spread and enhanced levels of PDE6α in treated mutant eyes. A single subretinal injection of AAV2/8-*TurboRFP* into the right eye of post-natal day (P) 5 *Pde6α*^{nmf363} mice and visualized at P55. Red fluorescence was overlayed onto a bright-field image of the whole mount for localization of fluorescence in respect to the entire retina. Scale bar: 4000 μm (**A**). A single subretinal injection of AAV2/8(Y733F)-*Rho-Pde6α* was performed in the right eye of P5 *Pde6α*^{nmf363} mice. Immunoblot analyses using PDE6α, RHO and β-actin antibodies were performed on retinal lysates from 2-month-old mice. β-Actin was used as a loading control. Forty micrograms of protein was loaded for both the treated and untreated mutant eyes. PDE6α antibody was not specific, and cross-reacted with the highly homologous PDE6β subunit (**B**). Immunoblot analyses using RHO and β-actin antibodies were performed on retinal lysates from a 2-month-old–treated mutant eye and a control B6 eye, along with an 11-month-old–treated mutant eye and control B6 eye. β-Actin was used as a loading control. Nine micrograms of protein was loaded for the 2-month-old samples and 20 μg of protein was loaded for the 11-month-old samples (**C**).

RP patients (OMIM 180071, 14). These mice mimic the clinical phenotype of recessive RP found in humans, where there is a progressive loss of photoreceptors and visual function, at a faster rate of degeneration than that which occurs in the *Pde6β*^{rd10} mouse model (15). No therapeutic strategies have been tested on these *Pde6α* models, to either correct or slow the progression of the disease phenotype.

In this study, we hypothesized that an AAV2/8 gene therapy vector can increase both photoreceptor survival and neuronal function in a mouse model with a mutation in the PDE6 α-subunit. We utilized an AAV vector designed to specifically express wild-type PDE6α in the *Pde6α* mutant rod photoreceptor cells through the *rhodopsin* gene promoter: AAV2/8(Y733F)-*Rho-Pde6α*. We delivered the AAV2/8(Y733F)-*Rho-Pde6α* virus into the right eye of *Pde6α*^{nmf363} mutant mice using a single subretinal injection. We then compared photoreceptor survival and visual function between the treated right eyes and the untreated left eyes of these mice.

RESULTS

AAV2/8(Y733F)-*Rho-Pde6α* vector map

The AAV2/8(Y733F)-*Rho-Pde6α* gene therapy vector was created using a pZac2.1 plasmid. The *Pde6α* complementary DNA (cDNA) fragment was inserted into this plasmid, along with 1.1 kb of the murine *rhodopsin* promoter, a Simian virus 40 (SV40) site, and poly(A) tail flanked by inverted terminal repeats (ITRs). This pZac2.1 plasmid with these sites inserted was used for packaging into the viral construct before subretinal injections (Fig. 1).

Retinal transduction of AAV2/8

To determine the transduction efficiency of AAV2/8 within the retina, a subretinal injection of AAV2/8-*TurboRFP* was administered to a litter of homozygous *Pde6α*^{nmf363} mutant mice. This vector expresses red fluorescent protein (RFP), which allows for the visualization of the cells transduced by the virus. After a single subretinal injection at post-natal day (P) five, RFP expression remained visible within the retina at P55, indicating that the virus was taken up by the retinal cells and survived for at least 2 months (Fig. 2A). RFP expression was detected within the portion of the retina that most likely correlated with the subretinal bleb, with only a minor scattering of fluorescence visible in other locations (Fig. 2A; blue circle).

PDE6α and RHO protein levels increased after treatment of *Pde6α*^{nmf363} mutant eyes

Since AAV2/8-*TurboRFP* transduced retinal cells after a single subretinal injection, we tested whether AAV2/8(Y733F)-*Rho-Pde6α* could express PDE6α in *Pde6α*^{nmf363} mutant mice. In untreated mutant eyes at 2 months of age, PDE6α protein was undetectable in the retinal lysate

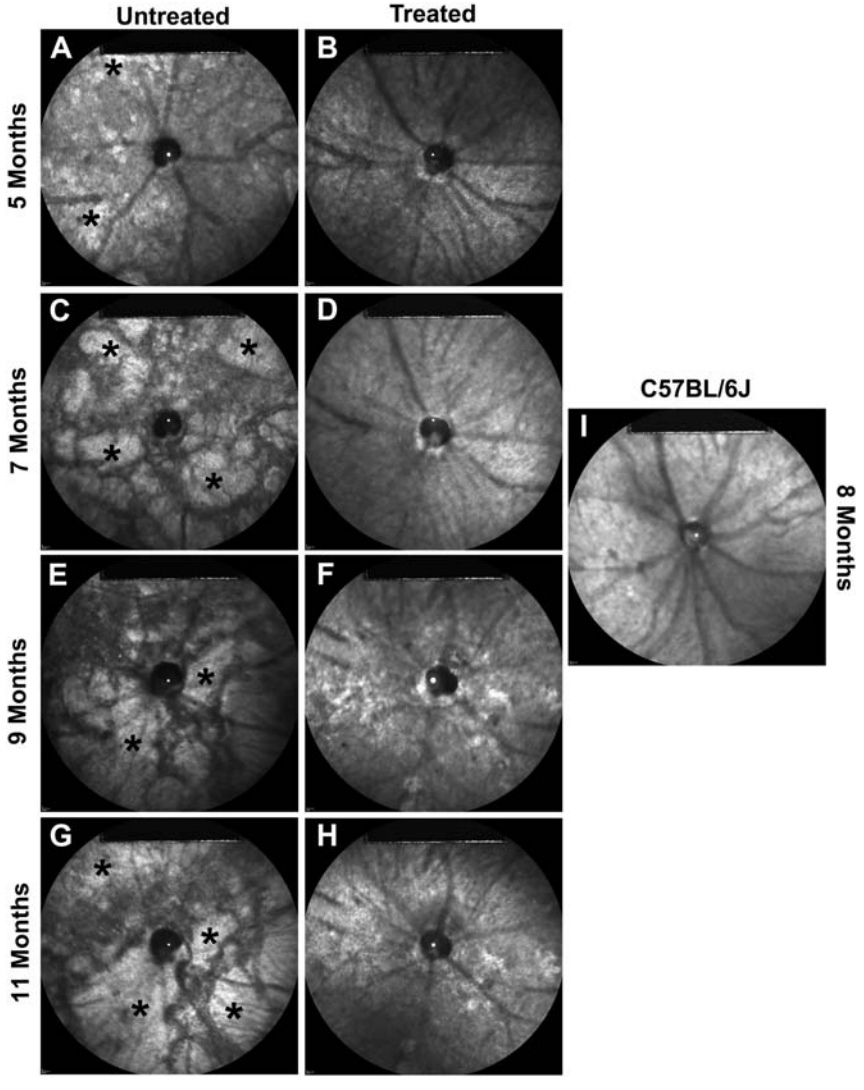

Figure 3. Delay of RPE atrophy after AAV2/8(Y733F)-*Rho-Pde6α* transduction. Representative infrared (IR) images of an untreated *Pde6α*^{nmf363} mutant eye at 5 (**A**), 7 (**C**), 9 (**E**) and 11 (**G**) months of age compared with the fellow-treated *Pde6α*^{nmf363} mutant eye at 5 (**B**), 7 (**D**), 9 (**F**) and 11 (**H**) months of age. Images for 5 and 7 months of age are taken from the same mouse, images from 9 and 11 months of age are taken from a second mouse for replication purposes. Representative IR image of a C57BL/6J control mouse at 8 months of age (**I**). Increased IR reflectance represents RPE atrophy (*). The attenuation of the arterioles is also arrested in the treated eyes at the ages examined. IR imaging was obtained at 790 nm absorption and 830 nm emission using a 55° lens. Images were taken of the central retina, with the optic nerve located at the center of the image and the site of the subretinal bleb along the lower left-hand quadrant.

(Fig. 2B). In contrast, PDE6α was observed in the retinal lysate of the mutant eye treated with the gene therapy vector (Fig. 2B). We also tested whether rhodopsin (RHO) is translated in the *Pde6α*^{nmf363} mutant mice, since RHO levels are indicative of the health of the photoreceptor outer segments (OS). The RHO protein levels were severely reduced in the untreated mutant eye, only detectable after over-exposure of the film, but RHO protein was detected at high levels in the treated mutant eye (Fig. 2B). We then compared the RHO levels in the treated mutant eyes at 2 and 11 months of age with that of a B6 control mouse (Fig. 2C). RHO is lower in the 2-month-old treated mutant eye, and RHO levels decline further by 11 months of age compared with a B6 control (Fig. 2C). In summary, the untreated mutant eye expressed undetectable levels and low levels of PDE6α and RHO, respectively, while the AAV2/8(Y733F)-*Rho-Pde6α*-treated mutant eye expressed higher levels of both PDE6α and RHO, although not as high as the levels of RHO in a B6 control mouse eye.

Delay of retinal pigment epithelial degeneration in treated *Pde6α*^{nmf363} mutant eyes

Since PDE6α protein is detectable after viral transduction and RHO protein levels suggest healthy photoreceptor neurons, we tested whether AAV2/8(Y733F)-*Rho-Pde6α* can rescue retinal pigment epithelial (RPE) degeneration visible upon fundus examination in RP patients. We examined infrared (IR) images of treated and fellow-untreated *Pde6α*^{nmf363} mutant eyes at 5, 7, 9 and 11 months of age (Fig. 3). A B6 mouse IR image was shown as a control at 8 months of age (Fig. 3I). At 5 months of age, the untreated mutant eye

shows the starting signs of RPE atrophy compared with the treated mutant eye (Fig. 3A and B; asterisks). Beginning at 7 months of age and continuing through 11 months of age, extensive RPE atrophy is visible in the untreated mutant eye (Fig. 3C, E and G; asterisks), while the treated mutant eye displays only a slight amount of RPE atrophy and appears to remain the same over time (Fig. 3D, F and H).

Increased PDE6α protein improved photoreceptor survival in *Pde6α*^{nmf363} mice

Since IR images displayed reduced RPE atrophy in treated *Pde6α*^{nmf363} mutant eyes compared with the fellow untreated eyes for at least 11 months, we tested whether AAV2/8(Y733F)-*Rho-Pde6α* is rescuing the photoreceptors in the *Pde6α*^{nmf363} mice. We examined histological sections from both the untreated and treated mutant eyes (Fig. 4). When viewing the treated retina of a 2-month-old *Pde6α*^{nmf363} mouse, the preservation of the photoreceptor cell bodies and OS is detectable in half of the retina (Fig. 4A).

To determine the extent and longevity of this rescue, we examined the outer nuclear layer (ONL) thickness of the rescued portion of the treated retina compared with both the un-rescued opposing side of the treated retina (as an internal control) and fellow untreated *Pde6α*^{nmf363} eyes in a longitudinal study (Fig. 4B). There were significantly more photoreceptor nuclei in the rescued portion of the treated eye (3.79 ± 4.21) when compared with the untreated fellow eye (1.44 ± 5.46) for the 6 months examined, and the opposing side of the treated retina showed a similar ONL thickness to the untreated fellow eye as would be expected with little to no rescue (Fig. 4B). The photoreceptor cell bodies declined between 1 and 2 months of age in the treated eye, then stabilized over the following months (Fig. 4B).

At 5 months of age, the ONL in mutant eyes was undetectable compared with a B6 control eye (Fig. 4C and E). In contrast, the ONL was not only detectable in the treated mutant eye compared with the untreated mutant eye (Fig. 4C and D), but it was ∼50% of the ONL thickness of the control B6 eye (Fig. 4D and E). Furthermore, OS were preserved in the treated regions of the mutant eye (Fig. 4D) compared with the untreated mutant eye (Fig. 4C), and of similar length as the B6 control (Fig. 4E). Thus, photoreceptors are present in the treated mutant eyes at a time when there is a loss of photoreceptors in the untreated mutant eyes, and this significant improvement in photoreceptor survival persists through at least 6 months of age.

Despite focal rescue of retinal structure adjacent to the injection site, global functional rescue is observed in *Pde6α*^{nmf363} mice

Since mutant photoreceptors survived after AAV2/8(Y733F)-*Rho-Pde6α* transduction, we tested whether these rescued photoreceptor cells were functional. We measured electroretinogram (ERG) responses in *Pde6α*^{nmf363} mice after AAV2/8(Y733F)-*Rho-Pde6α* transduction beginning at 1 month of age (Fig. 5). By 2 months of age when the untreated mutant eye lost almost all visual response, the treated mutant eye retained a strong visual response, although with a lower maximum *b*-wave amplitude and reduced *a*-wave amplitude than that of a control wild-type B6 mouse (Fig. 5A). At 5 months of age, the treated mutant eye retained an ∼100 μV *b*-wave amplitude, similar to that observed at 2 months of age (Fig. 5B). Each month, the overall visual response was significantly enhanced in the treated eyes

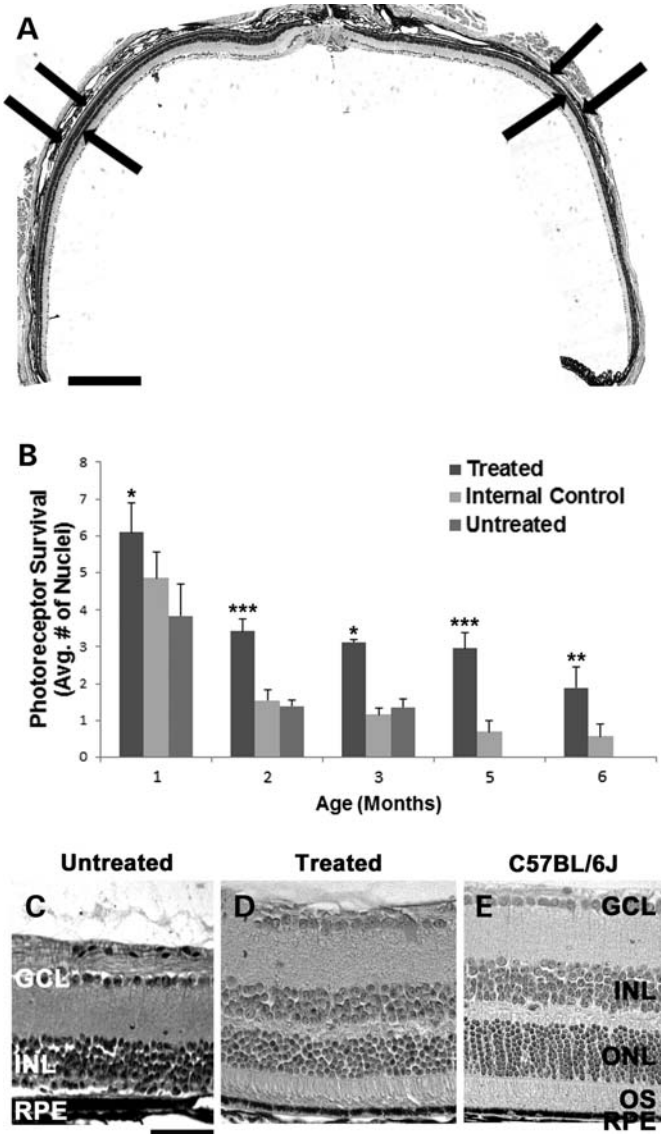

Figure 4. Improved photoreceptor survival after AAV2/8(Y733F)-*Rho-Pde6α* transduction. H&E stained retinal section of a 2-month-old-treated *Pde6α*^{nmf363} mouse eye (**A**). Images were composited together to show entire retina. Arrows show ONL and OS regions. Scale bar: 1000 μm. Quantification of the thickness of the ONL by counting the columns of photoreceptor nuclei in the rescued half of the treated retina, the un-rescued half of the treated retina (labeled internal control) and fellow-untreated eyes from 1 to 6 months of age (**B**). Error bars show SEM for each time point and the significance was calculated for the rescued half of the treated retina compared with the untreated fellow eyes using ratio paired *t*-test analysis. $N \geq 3$ mice. H&E stained retinal section of a 5-month-old-untreated *Pde6α*^{nmf363} mouse retina (**C**), the fellow *Pde6α*^{nmf363} mouse retina treated with AAV2/8(Y733F)-*Rho-Pde6α* (**D**) and a B6 control mouse (**E**). Scale bar: 600 μm. GCL, ganglion cell layer; INL, inner nuclear layer; ONL, outer nuclear layer; OS, outer segments; RPE, retinal pigment epithelium. $^{*}p < 0.05$; $^{**}p < 0.01$; $^{***}p < 0.001$.

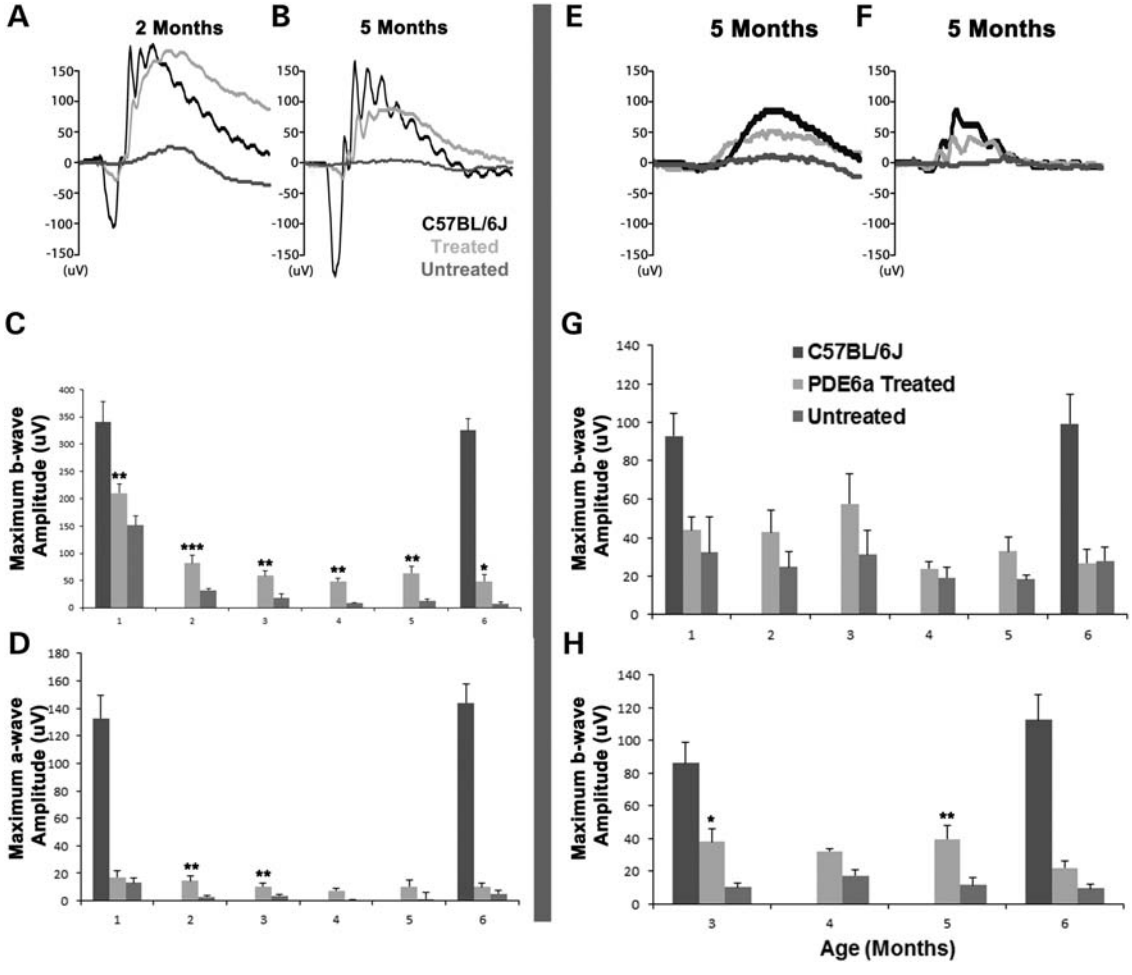

Figure 5. Rescued visual function after AAV2/8(Y733F)-*Rho-Pde6α* transduction. Representative scotopic maximum ERG traces for a B6 control mouse (black), the treated eye (light grey) and the untreated eye (dark grey) of a *Pde6α*^{nmf363} mouse at 2 months of age (**A**), and 5 months of age (**B**). Maximum scotopic *b*-wave amplitudes in a B6 mouse, the treated *Pde6α*^{nmf363} eyes and fellow-untreated eyes monthly between 1 and 6 months of age (**C**). Maximum scotopic photoreceptor-mediated *a*-wave amplitudes (shown as positive values) in a B6 mouse, the treated *Pde6α*^{nmf363} eyes and fellow-untreated eyes monthly between 1 and 6 months of age (**D**). Representative scotopic dim light rod-specific ERG traces of a B6 control mouse (black), the treated eye (light grey) and the untreated eye (dark grey) of a *Pde6α*^{nmf363} mouse at 5 months of age (**E**), and representative photopic single flash cone-mediated ERG traces for a B6 control mouse (black), the treated eye (light grey) and the untreated eye (dark grey) of a *Pde6α*^{nmf363} mouse at 5 months of age (**F**). Dim light rod-specific scotopic *b*-wave amplitudes in a B6 mouse, the treated *Pde6α*^{nmf363} eyes and fellow-untreated eyes monthly between one and 6 months of age (**G**). Photopic cone-specific *b*-wave amplitudes in a B6 mouse, the treated *Pde6α*^{nmf363} eyes and fellow-untreated eyes from 3 to 6 months of age (**H**). B6 mouse ERG results did not vary over the 6-month testing period so only the first and last results are shown in the charts. Error bars show SEM for each time point and the significance was calculated using the ratio paired *t*-test analysis. $N \geq 3$ mice. $^{*}p < 0.05$; $^{**}p < 0.01$; $^{***}p < 0.001$.

compared with untreated fellow eyes and this lasted through 6 months of age, the last age examined (Fig. 5C).

Furthermore, since recessive RP caused by mutations in PDE6α is a rod-cone dystrophic disease, we tested whether the rod- and cone-specific visual responses were improved after a single subretinal injection with AAV2/8(Y733F)-*Rho-Pde6α.* The maximum ERG *a*-wave, which is a photoreceptor-dominated response, although substantially decreased in the ERG traces (Fig. 5A and B), was increased in our treated mutant eyes compared with fellow untreated eyes over the 6-month period (Fig. 5D). Additionally, ERG responses from a dim light rod-only stimulation showed some waveforms where, at 5 months of age, the treated mutant eye retained a strong rod response, although with a lower maximum amplitude than that of a control wild-type B6 mouse (Fig. 5E). However, not all treated mice displayed a strong dim light ERG trace, and between 2 and 5 months of age, the treated mutant eyes showed improved rod-specific *b*-wave responses over the fellow untreated mutant eyes, but these were not significant (Fig. 5G).

Lastly, even if only a relatively small number of rod photoreceptor cells were functional after treatment, cone cells may still survive and function in these mice, so we tested for cone cell-specific visual function. We used light-adapted photopic ERG responses, which are cone-specific, and found that at 5 months of age, the traces from the treated mutant mice displayed a strong cone cell visual response compared with the untreated eye, which lost almost all visual response (Fig. 5F). Additionally, the waveforms from the treated mutant eye were similar to that of a B6 control mouse, and

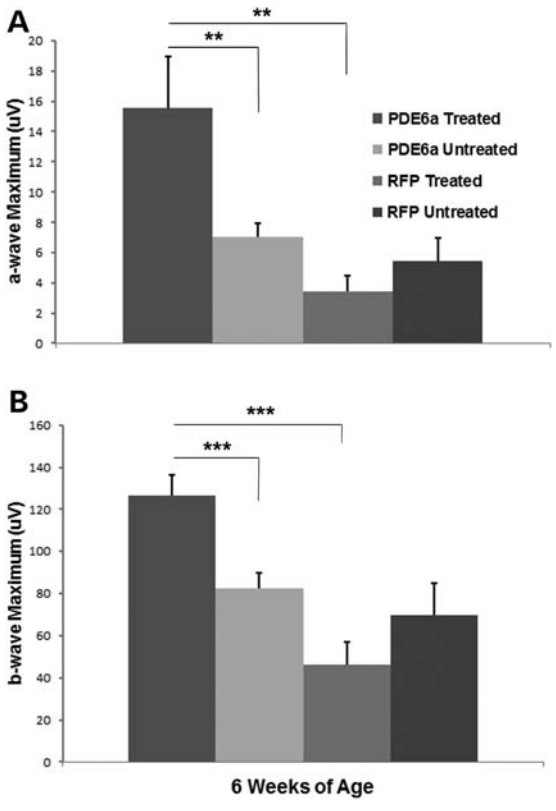

Figure 6. No rescued visual function from a control vector injection. Maximum photoreceptor-specific *a*-wave amplitudes (shown as positive values) in 6-week-old treated *Pde6α*^{nmf363} eyes compared with their fellow-untreated eyes and *Pde6α*^{nmf363} mice treated with AAV2/8-*TurboRFP* alone (**A**). Maximum *b*-wave amplitudes in 6-week-old-treated *Pde6α*^{nmf363} eyes compared with their fellow-untreated eyes and *Pde6α*^{nmf363} mice treated with AAV2/8-*TurboRFP* alone (**B**). Error bars show SEM for each time point and the significance was calculated using ratio paired and two-tailed *t*-test analyses. $N \geq 8$ mice. $^{*}p < 0.05$; $^{**}p < 0.01$; $^{***}p < 0.001$.

only slightly reduced in amplitude (Fig. 5F). The cone cell visual responses were enhanced in our treated mutant eyes compared with untreated fellow eyes through at least 6 months of age, the last date tested (Fig. 5H). Taken together, our data suggest that treatment with AAV2/8(Y733F)-*Rho-Pde6α*, and its subsequent increase of PDE6α levels, rescues photoreceptor survival and inner retina visual function for at least 6 months in the *Pde6α*^{nmf363} mouse.

We also tested if injection of the viral vector alone is able to cause a functional restoration of the photoreceptor cells. We analyzed ERG responses from the AAV2/8-*TurboRFP* treated *Pde6α*^{nmf363} mice, to ensure that the injection of the AAV2/8 virus alone does not cause any functional rescue effect (Fig. 6). At 6 weeks of age, the photoreceptor-specific and overall visual function in the AAV2/8-*TurboRFP* treated and untreated eyes were not significantly different (Fig. 6). In contrast, the AAV2/8(Y733F)-*Rho-Pde6α* treated mutant eyes displayed significant improvement over the untreated eyes or those treated with the AAV2/8-*TurboRFP* virus alone (Fig. 6). Thus, the AAV2/8(Y733F)-*Rho-Pde6α* vector-induced increase in PDE6α protein is likely responsible for the significant rescue in visual function through 6 months of age (Figs. 3–5).

DISCUSSION

Only recently, attempts at using AAV2/8 gene therapy to functionally rescue mouse models of RP, in particular one *Pde6β* mouse model, has shown long-term rescue effects (13). Lentiviral, or other AAV serotypes, can delay photoreceptor degeneration in multiple *Pde6β* mouse models, but long-term efficacy has not been found in the majority of the reported studies (5–12). Although one AAV gene therapy case has now shown 6-month rescue in a slower photoreceptor degeneration *Pde6β* mouse model, studies have not been conducted on animal models with mutations in the α-subunit of PDE6 to ameliorate the disease progression.

Here, we applied AAV-based gene therapy that can rescue photoreceptor degeneration and restore neuronal function in a *Pde6α*^{nmf363} mouse model of recessive RP. We demonstrate that after a single subretinal injection of AAV2/8(Y733F)-*Rho-Pde6α* into the *Pde6α*^{nmf363} mouse, the phenotype can be both structurally and functionally rescued. Sakamoto *et al.* showed that PDE6α protein was severely diminished in P12 *Pde6α*^{nmf363} mutant mice (14), and we found that PDE6α protein was undetectable in the 2-month-old *Pde6α*^{nmf363} mutant retinal lysates. This suggests that the PDE6α protein levels found in the treated mutant eye most likely came from the cells that were transduced by the AAV2/8(Y733F)-*Rho-Pde6α* vector. Additionally, the small amount of PDE6α protein provided by the viral injection protected the RHO protein expression in the treated *Pde6α*^{nmf363} mutant eye, since it was undetectable in the untreated mutant eye. Thus, AAV2/8(Y733F)-*Rho-Pde6α* partially rescues mutant photoreceptors in treated eyes as evidenced by the increase in both PDE6α levels, directly, and RHO levels, indirectly, both of which are necessary to correct the recessive RP disease phenotype in our *Pde6α*^{nmf363} mouse model.

Furthermore, our study replicates the results published by Sakamoto *et al.* on the retinal degenerative phenotype of the *Pde6α*^{nmf363} mouse model and extends the observation beyond 1 month of age (14). We found that the RHO protein levels were diminished by 2 months of age, suggesting a loss of photoreceptor cells, which correlates with histological sections showing that the ONL photoreceptor cell nuclei decreased to approximately one to two cell thickness after 2 months of age. Additionally, a complete loss of ONL photoreceptor cell nuclei occurred in the mutant eye by 5 months of age. ERGs displayed similar findings, where the visual response was severely attenuated after 2 months of age, and cone cell-specific ERG responses declined dramatically by 5 months of age. Upon IR examination, RPE atrophy begins around 5 months of age, after the loss of the ONL and OS in the mutant eyes, and this RPE atrophy increases dramatically by 7 months of age through 11 months of age, the latest time point that was studied.

Effective photoreceptor rescue after AAV2/8(Y733F)-*Rho-Pde6α* transduction is confined to the location of the subretinal bleb, and the variability of the size of the subretinal bleb can account for gene transfer and therapeutic efficiency between different eyes. Photoreceptor survival occurred along one half of the treated retina (Fig. 4), most likely on the side where the gene therapy injection site was located and the subretinal bleb was formed (Fig. 2A). This correlates with the

ERG results, where the treated *Pde6α*^{nmf363} mutant mice had enhanced visual responses long-term, at ∼20% of that found in a B6 mouse (Fig. 5).

Additionally, the amount of cells that are transduced by the virus is variable. The representative ERG waveforms (Fig. 5A, B, E and F) display the ERG responses under each condition in a mouse with a strong visual response. The charts shown in Figure 5C, D, G and H take into account all of the mice at each time examined, and this variation in the size of the subretinal bleb during the surgical procedure may account for the strength of significance and deviation in these charts.

For the dim light rod-specific ERG responses, statistical analysis of the treated and untreated eyes demonstrated no significant differences at any time point in this pooled set of treated eyes (*N* ranges from 3–8 mice per time point), although the treated mutant eyes showed some improvement over the untreated mutant eyes from 2 to 5 months of age. Additionally, we found three mice with evidence of rod-specific ERG responses much higher than the untreated eyes (Fig. 5E), and these three mice showed comparable rod-specific ERG responses at multiple time points in the 6-month study period. One interpretation of this result is that a threshold level of transduction (number of rods transduced) is able to produce a more effective rescue of rod function and that the transduction levels of the majority of mice were below this level. This is likely due to variation during the surgical procedure. Alternatively, the variable ability of the vector to produce detectable rod-specific ERG rescue may be related to the capability of the vector to sustain PDE6α expression and/or survival of the transduced rods.

Additionally, we found that the ONL and the OS declined in the treated eyes until 2 months of age, and then remained at a similar thickness through 6 months of age. This suggests a halt in the progression of photoreceptor death after transduction with AAV2/8(Y733F)-*Rho-Pde6α,* where the treated eye has photoreceptor survival in the location of the subretinal bleb, but the remaining half of the retina continues to degenerate. This effect was also seen in the ERG results, where ERG traces decline until 2 months of age, then have a similar visual response to those at 6 months of age in the same mouse (Fig. 4D and E, Fig. 5A and B). At 2 months of age, the ERG tracing for the treated mutant eye has a similar maximum *b*-wave amplitude to that of a control B6 mouse; however, a decreased *a*-wave amplitude as would be expected with the loss of photoreceptor cells in the unrescued half of the treated retina. The strength of the *b*-wave amplitude is likely due to the remaining photoreceptors and the inner retinal cells of the eye. By 5 months of age, the ERG tracing for the treated mutant eye retains the strong visual response from the remaining photoreceptors and inner retinal cells, but has a reduced maximum *b*-wave amplitude compared with the B6 control mouse response, which correlates with the thinner ONL seen in Figure 4D compared with Figure 4E, as the unrescued half of the treated retina is fully degenerated.

However, despite focal rescue of retinal structure adjacent to the injection site, we achieved remarkable global functional restoration as assessed by ERG that lasted over 6 months of age, a quarter of the mouse lifespan. RHO levels declined by 11 months of age in the treated mutant eyes; however, IR imaging showed strong RPE atrophy in untreated mutant eyes, but healthy fundus images of the fellow treated mutant eyes through 11 months of age; half of the mouse lifespan. Although only half of the retina retains photoreceptor cells after subretinal injection, it appears that these cells are enough to protect the treated eye from the secondary remodeling effects that occur after photoreceptor cell death in RP, such as RPE atrophy.

'Sham' injections have been found to produce rescue effects that last through a 6-month testing period in the Royal College of Surgeons (RCS) rat model of RP (16,17). In RCS rats, a washing away of accumulated OS debris during the injection procedure is the likely cause of the noticeable rescue effects. Injection of our AAV2/8 'blank' vector alone did not cause functional rescue in the *Pde6a*^{nmf363} mouse model; therefore, the rescue effects found for 6 months in this study are specific to AAV2/8(Y733F)-*Rho-Pde6α* transgene transduction.

Early rod photoreceptor dysfunction characterizes diseases that include RP and AMD. The reduction of PDE6 function is a common denominator in 36 000 cases of photoreceptor degeneration. Our study indicates that it may be possible to develop treatments based on correcting PDE6 levels using gene therapy vectors. Additional studies, however, are needed to examine the full duration of rescue, the timing of injections in respect to disease progression, the possibility of multiple injection sites, and re-injections if the virus begins to lose its ability to rescue the cells. While these studies need to be conducted, our results indicate a significant treatment potential for both photoreceptor cell survival and functional rescue in mice carrying a mutant allele of *Pde6α*. Ultimately, the results from this study demonstrates potential for using gene therapy modifications to treat RP in the Cardigan Welsh Corgi, a dog model with a mutation in *PDE6α*, and in human patients with RP caused by PDE6α mutations.

MATERIALS AND METHODS

Mouse lines and husbandry

C57BL/6J-*Pde6α*$^{nmf363/nmf363}$, with a D670G mutation, herein referred to as *Pde6α*^{nmf363}, mice were obtained from the Jackson Laboratory (Bar Harbor, ME, USA). Mice were maintained in the Columbia University Pathogen-free Eye Institute Annex Animal Care Services Facility under a 12/12-h light/dark cycle. All experiments were approved by the local Institutional Animal Care and Use Committee (IACUC) under protocol #AAAB-4306. Mice were used in accordance with the Statement for the Use of Animals in Ophthalmic and Vision Research of the Association for Research in Vision and Ophthalmology, as well as the Policy for the Use of Animals in Neuroscience Research of the Society for Neuroscience. *Pde6α*^{nmf363} mice used in this study were bred from a colony of mice that has been previously reported (14). *Pde6α*^{nmf363} are coisogenic in the C57BL/6J (B6) background; therefore, age-matched B6 mice were used as experimental controls (The Jackson Laboratory).

Construction of AAV vectors

AAV serotype 2/8 capsids containing a point mutation in surface-exposed tyrosine residues, AAV2/8(Y733F), exhibit higher transduction efficiency in photoreceptors and a faster onset of expression than other AAV serotypes when delivered into the subretinal space of the eye (13). Therefore, these vectors were used for packaging our *Pde6α* construct. Vector plasmids were constructed by inserting 1.1 kb of the murine *rhodopsin* promoter region [Ensembl, rhodopsin, chromosome 6: (115, 930, 881–115, 931, 988); Ensembl, rhodopsin, ATG = 1: (−1125, −17)] and a full-length murine *Pde6α* cDNA fragment into the pZac2.1 plasmid to generate pZac2.1.m*Rhodopsin*.m*Pde6α*.SV40 (18). AAV vectors were created, packaged and purified at the Penn Vector Corporation, to become AAV2/8(Y733F).m*Rhodopsin*.m*Pde6α*.SV40 (University of Pennsylvania, PA, USA). The AAV2/8(Y733F).m*Rhodopsin*.m*Pde6α*.SV40 vector will be referred to as AAV2/8(Y733F)-*Rho-Pde6α* in this publication. AAV2/8.*CMV.TurboRFP*.RBG was purchased from the Penn Vector Corporation as the AAV serotype control and will be referred to as AAV2/8-*TurboRFP* in this publication.

Transduction of AAV vectors

To increase levels of wild-type PDE6α, we injected AAV2/8(Y733F)-*Rho-Pde6α* (0.7μl, 1.26e13 genome copy (GC)/ml) into the subretinal space of the right eye of *Pde6α*^{nmf363} mice at post-natal day (P) 5. AAV2/8-*TurboRFP* (0.7 μl, 7.28e12 GC/ml) was injected into the subretinal space of the right eye of *Pde6α*^{nmf363} mice at P5 for control experiments. Virus particles were injected at the 6 o'clock position of the eye, ∼1.5 mm from the limbus, to produce a subretinal bleb in the mid-periphery of the retina. The left eyes of all mice were kept as a matched control for experimental analyses. Anesthesia and surgery were performed as previously described (6).

Whole mount analysis

Mice were euthanized according to the established IACUC guidelines. Eyes were enucleated and placed in 2% paraformaldehyde for 1 h at room temperature. The optic nerve, cornea and lens were removed. The whole eyecup was then flattened by means of four radial cuts extending out from the optic nerve and mounted with mounting medium (Vectashield, Burlingame, CA, USA). RFP visualization was achieved by fluorescence microscopy, and bright-field imaging was used to visualize the whole retina (Leica DM 5000B microscope). Pictures were taken at 2.5× magnification using the Leica Application Suite Software (Leica Microsystems Inc., Germany).

Immunoblot analysis

Retinas were homogenized in 10% sodium dodecyl sulfate (SDS) by brief sonication and denatured at 100°C for 5 min. Following centrifugation, the total protein content per sample was measured using the DC protein assay method (Bio-Rad Laboratories, Hercules, CA, USA). Proteins were separated by SDS polyacrylamide gel electrophoresis. The samples were then transferred to nitrocellulose membranes, which were blocked in 3% bovine serum albumin (BSA; Santa Cruz Biotechnology, Santa Cruz, CA, USA), 150 mmol/l NaCl, 100 mmol/l Tris (pH 7.4) and 0.5% Tween-20 (BSA-TTBS). Membranes were incubated with either anti-PDE6α (1:300, Abcam), rhodopsin (1D4) (1:500, Santa Cruz) or rabbit anti-cytoskeletal actin (1:300, Bethyl) antibodies in BSA-TTBS. After washing in TTBS, filters were incubated with goat anti-rabbit or goat anti-mouse-conjugated horseradish peroxidase secondary antibodies (1:20 000, Santa Cruz Biotechnology). After washing, antibody complexes were visualized by a chemiluminescence detection kit (Immobilon Western, Millipore Corporation, Billerica, MA, USA) and a Kodak BioMax film (Kodak, Rochester, NY, USA).

Infrared Imaging

IR fundus imaging was obtained with the Spectralis scanning laser confocal ophthalmoscope (Heidelberg Engineering, Carlsbad, CA, USA). IR imaging was obtained at 790 nm absorption and 830 nm emission using a 55° lens. Images were taken of the central retina, with the optic nerve located in the center of the image and the site of the subretinal bleb along the lower left-hand quadrant.

Histochemical analyses

Mice were sacrificed and the eyes enucleated as previously described (19). Excalibur Pathology, Inc. prepared Hematoxylin & Eosin retinal sections. The morphology of photoreceptors and the amount of photoreceptor cell nuclei of AAV2/8(Y733F)-*Rho-Pde6α*-treated eyes were compared with the untreated fellow eyes. Quantification of photoreceptor nuclei was conducted on several sections that contained the optic nerve, as follows: the distance between the optic nerve and the ciliary body was divided into four, approximately equal, quadrants. Three columns of nuclei (how many cell nuclei thick) were counted within each single quadrant. These counts were then used to determine the average thickness of the ONL for each individual animal at each time. For the treated eyes, the rescued half of the treated retina between the optic nerve and the ciliary body was quantified in this manner, with the opposite side of the retina, between the optic nerve and the ciliary body, being quantified similarly and considered the unrescued half of the treated mutant eye (the internal control). Averages and standard deviations were calculated from animals for each time point using ratio paired *t*-test statistical analyses with statistical significance set at $P < 0.05$. Sectioning proceeded along the long axis of the segment, so that each section contained upper and lower retina as well as the posterior pole.

Electroretinograms

Mice were dark-adapted overnight, manipulations were conducted under dim red light illumination, and recordings were made using Espion ERG Diagnosys equipment (Diagnosys

LLL, Littleton, MA, USA). Adult B6 control mice were tested at the beginning of each session to ensure equal readouts from the electrodes for both eyes before testing the experimental mice. Pupils were dilated using topical 2.5% phenylephrine hydrochloride and 1% tropicamide (Akorn Inc., Lakeforest, IL, USA). Mice were anesthetized by intraperitoneal injection of 0.1 ml/10 g body weight of anesthesia [1 ml ketamine 100 mg/ml (Ketaset III, Fort Dodge, IA, USA) and 0.1 ml xylazine 20 mg/ml (Lloyd Laboratories, Shenandoah, IA, USA) in 8.9 ml PBS]. Body temperature was maintained at 37°C using a heating pad during the procedure. Hand-made electrodes were placed upon the corneas and gonioscopic prism solution (Alcon Labs, Inc., Fort Worth, TX, USA) was applied to each eye. Both eyes were recorded simultaneously. A total of 40–60 responses were averaged for each trial. All further detail on the ERG method has been described previously (20,21). We measured scotopic dim light maximal *b*-wave ERG responses to assess rod-only responses, scotopic maximal *b*-wave ERG responses to assess inner retina function, scotopic maximal *a*-wave ERG responses to assess photoreceptor-specific function, and photopic maximal b-wave ERG responses to assess cone-specific function. Maximal responses were taken from the Espion readout in microvolts and quantified using ratio paired *t*-test statistical analyses with statistical significance set at $P < 0.05$.

AUTHORS' CONTRIBUTIONS

K.J.W. and S.H.T. designed research; P.M.N. contributed mice; K.J.W. and J.S.P. performed research; K.J.W., R.J.D. and S.H.T. analyzed data; K.J.W., S.H.T., P.M.N. and R.J.D. wrote the paper.

ACKNOWLEDGEMENTS

We are grateful for Dr Chyuan-Sheng Lin's pulled capillary needles for use in this study.

Conflict of Interest statement. The authors declare no competing financial interests.

FUNDING

Imaging and animal facilities are supported by the National Institute of Health Core grant 5P30EY019007 and NCI Core grant 5P30CA013696 and unrestricted funds from Research to Prevent Blindness, New York, NY, USA. The Bernard and Shirlee Brown Glaucoma Laboratory is supported by R01EY018213, Department of Defense, Fort Detrick, MD, grant TS080017-W81XWH-09-1-0575, the Foundation Fighting Blindness, Schneeweiss Stem Cell Fund, and the Tistou and Charlotte Kerstan Foundation. S.H.T. is a member of the RD-CURE Consortium, Fellow of the Burroughs-Wellcome Program in Biomedical Sciences, and has been supported by the Bernard Becker Association of University Professors in Ophthalmology Research to Prevent Blindness Award, Dennis W. Jahnigen Award of the American Geriatrics Society, Joel Hoffman Scholarship, Schneeweiss Stem Cell Fund, Irma T. Hirschl Charitable Trust, Crowley Family Fund, Barbara and Donald Jonas Family Fund and Professor Gertrude Rothschild Stem Cell Foundation. K.J.W. is supported by NIH training grants 5T32EY013933 and 5T32DK007647-20. P.M.N. is supported by grant EY016501.

REFERENCES

1. Dryja, T.P. and Berson, E.L. (1995) Retinitis pigmentosa and allied diseases: Implications of genetic heterogeneity. *Invest. Ophthalmol. Vis. Sci.*, **36**, 1197–1200.
2. Daiger, S.P., Bowne, S.J. and Sullivan, L.S. (2007) Perspective on genes and mutations causing retinitis pigmentosa. *Arch. Ophthalmol.*, **125**, 151–158.
3. Baehr, W., Devlin, M.J. and Applebury, M.L. (1979) Isolation and characterization of cGMP phosphodiesterase from bovine rod outer segments. *J. Biol. Chem.*, **254**, 11669–11677.
4. Fung, B.K., Young, J.H., Yamane, H.K. and Griswold-Prenner, I. (1990) Subunit stoichiometry of retinal rod cGMP phosphodiesterase. *Biochemistry*, **29**, 2657–2664.
5. Tosi, J., Sancho-Pelluz, J., Davis, R.J., Hsu, C.W., Wolpert, K.V., Sengillo, J.D., Lin, C.S. and Tsang, S.H. (2011) Lentivirus-mediated expression of cDNA and shRNA slows degeneration in retinitis pigmentosa. *Exp. Biol. Med.*, **236**, 1211–1217.
6. Davis, R., Tosi, J., Janisch, K.M., Kasanuki, J.M., Wang, N.K., Kong, J., Tsui, I., Cillufo, M., Woodruff, M.L., Fain, G.L. *et al.* (2008) Functional rescue of degenerating photoreceptors in mice homozygous for a hypomorphic cGMP phosphodiesterase 6 allele (Pde6bH620Q). *Invest. Ophthalmol. Vis. Sci.*, **49**, 5067–5076.
7. Kumar-Singh, R. and Farber, D.B. (1998) Encapsidated adenovirus mini-chromosome-mediated delivery of genes to the retina: application to the rescue of photoreceptor degeneration. *Hum. Mol. Genet.*, **7**, 1893–1900.
8. Bennett, J., Tanabe, T., Sun, D., Zeng, Y., Kjeldbye, H., Gouras, P. and Maguire, A.M. (1996) Photoreceptor cell rescue in retinal degeneration (rd) mice by *in vivo* gene therapy. *Nat. Med.*, **2**, 649–654.
9. Jomary, C., Vincent, K.A., Grist, J., Neal, M.J. and Jones, S.E. (1997) Rescue of photoreceptor function by AAV-mediated gene transfer in a mouse model of inherited retinal degeneration. *Gene Ther.*, **4**, 683–690.
10. Takahashi, M., Miyoshi, H., Verma, I.M. and Gage, F.H. (1999) Rescue from photoreceptor degeneration in the rd mouse by human immunodeficiency virus vector-mediated gene transfer. *J. Virol.*, **73**, 7812–7816.
11. Lem, J., Flannery, J.G., Li, T., Applebury, M.L., Farber, D.B. and Simon, M.I. (1992) Retinal degeneration is rescued in transgenic rd mice by expression of the cGMP phosphodiesterase beta subunit. *Proc. Natl Acad. Sci. USA*, **89**, 4422–4426.
12. Pang, J.J., Boye, S.L., Kumar, A., Dinculescu, A., Deng, W., Li, J., Li, Q., Rani, A., Foster, T.C., Chang, B. *et al.* (2008) AAV-mediated gene therapy for retinal degeneration in the rd10 mouse containing a recessive PDEbeta mutation. *Invest. Ophthalmol. Vis. Sci.*, **49**, 4278–4283.
13. Pang, J.J., Dai, X., Boye, S.E., Barone, I., Boye, S.L., Mao, S., Everhart, D., Dinculescu, A., Liu, L., Umino, Y. *et al.* (2011) Long-term retinal function and structure rescue using capsid mutant AAV8 vector in the rd10 mouse, a model of recessive retinitis pigmentosa. *Mol. Ther.*, **19**, 234–242.
14. Sakamoto, K., McCluskey, M., Wensel, T.G., Naggert, J.K. and Nishina, P.M. (2009) New mouse models for recessive retinitis pigmentosa caused by mutations in the Pde6a gene. *Hum. Mol. Genet.*, **18**, 178–192.
15. Gargini, C., Terzibasi, E., Mazzoni, F. and Strettoi, E. (2007) Retinal organization in the retinal degeneration 10 (rd10) mutant mouse: a morphological and ERG study. *J. Comp. Neurol.*, **500**, 222–238.
16. Wen, R., Song, Y., Cheng, T., Matthes, M.T., Yasumura, D., LaVail, M.M. and Steinberg, R.H. (1995) Injury-induced upregulation of bFGF and CNTF mRNAs in the rat retina. *J. Neurosci.*, **15**, 7377–7385.
17. Woch, G., Aramant, R.B., Seiler, M.J., Sagdullaev, B.T. and McCall, M.A. (2001) Retinal transplants restore visually evoked responses in rats with photoreceptor degeneration. *Invest. Ophthalmol. Vis. Sci.*, **42**, 1669–1676.
18. Baehr, W., Champagne, M., Lee, A.K. and Pittler, S.J. (1991) Complete cDNA sequences of mouse rod photoreceptor cGMP phosphodiesterase

alpha- and beta-subunits, and identification of beta'-, a putative beta-subunit isozyme produced by alternative splicing of the beta-subunit gene. *FEBS Lett.*, **278**, 107–114.
19. Tsang, S.H., Burns, M.E., Calvert, P.D., Gouras, P., Baylor, D.A., Goff, S.P. and Arshavsky, V.Y. (1998) Role of the target enzyme in deactivation of photoreceptor G protein *in vivo*. *Science*, **282**, 117–121.
20. Hood, D.G. and Birch, D.G. (1994) Rod phototransduction in retinitis pigmentosa: estimation and interpretation of parameters derived from the rod a-wave. *Invest. Ophthalmol. Vis. Sci.*, **35**, 2948–2961.
21. Hood, D.C. and Birch, D.G. (1992) A computational model of the amplitude and implicit time of the b-wave of the human ERG. *Vis. Neurosci.*, **8**, 107–126.